Fast Track Communications

IOP Publishing

Journal of Physics D: Applied Physics

J. Phys. D: Appl. Phys. **48** (2015) 152001 (6pp)

doi:10.1088/0022-3727/48/15/152001

Fast Track Communications

Scalable control of graphene growth on 4H-SiC C-face using decomposing silicon nitride masks

Renaud Puybaret[1,2], John Hankinson[3], James Palmer[3], Clément Bouvier[3], Abdallah Ougazzaden[1,2], Paul L Voss[1,2], Claire Berger[3,4] and Walt A de Heer[3]

[1] School of Electrical and Computer Engineering, Georgia Institute of Technology, Atlanta, GA 30332, USA
[2] Georgia Tech—CNRS UMI 2958, 2-3 Rue Marconi, 57070 Metz, France
[3] School of Physics, Georgia Institute of Technology, Atlanta, GA 30332, USA
[4] CNRS-Institute Néel, BP 166, 38042 Grenoble, Cedex 9, France

E-mail: renaudpuybaret@gmail.com

Received 13 February 2015, revised 26 February 2015
Accepted for publication 3 March 2015
Published 25 March 2015

Abstract

Selective epitaxial graphene growth is achieved in pre-selected areas on the 4H-SiC$(000\bar{1})$ C-face with a SiN masking method. The mask decomposes during the growth process leaving a clean, resist free, high temperature annealed graphene surface, in a one-step process. Depending on the off-stoichiometry composition of a $Si_{3+x}N_4$ mask evaporated on SiC prior to graphitization, the number of layers on the C-face increases (Si-rich) or decreases (N-rich). Graphene grown in masked areas shows excellent quality as observed by Raman spectroscopy, atomic force microscopy and transport data.

Keywords: graphene, scalable, control, growth, silicon nitride, silicon carbide

(Some figures may appear in colour only in the online journal)

Epitaxial graphene (EG) on SiC shows compelling physical characteristics such as ballistic transport in nanoribbons [1], half-eV band-gap structures [2], metrology standard quantum-Hall effect [3] and high frequency transistors [4, 5]. Epitaxial graphene on the 4H-SiC$(000\bar{1})$ C-face shows high electronic mobility [6], up to 10^6 cm^2 Vs^{-1} at room temperature for the inner layers [7], a record high maximum oscillation frequency transistor operation [5] and two-orders of magnitude longer spin diffusion length than any other material [8]. Because SiC is a monocrystalline semiconducting industrial substrate, epitaxial graphene on SiC is directly compatible with established scalable device fabrication techniques, making it interesting for advanced electronic devices as well [9, 10]. Patterning of clean graphene devices is key for the study of physical properties and devices. In most cases, 2D graphene is first grown then patterned by oxygen plasma. However resist residues, that can cause unintentional doping or scattering, are difficult to eliminate. Selective area growth of graphene is a more straightforward approach, as it could in principle provide patterned structures directly during growth. Local control of graphene growth has been previously achieved by AlN capping [11], ion implantation of Au or Si [12], or on side-wall nanoribbons [13]. However, in these cases the foreign atoms remain in the system or the graphene is limited to very narrow structures.

In this article, we report on a method for controlling graphene growth selectivity down to the sub-micron level in a one-step process with a vanishing mask. We find that deposition of a 120–50 nm-thick silicon nitride mask on C-face $(000\bar{1})$ 4H-SiC prior to graphitization modifies the number of multi-layer epitaxial graphene (MEG) sheets. The silicon

 © 2015 IOP Publishing Ltd Printed in the UK

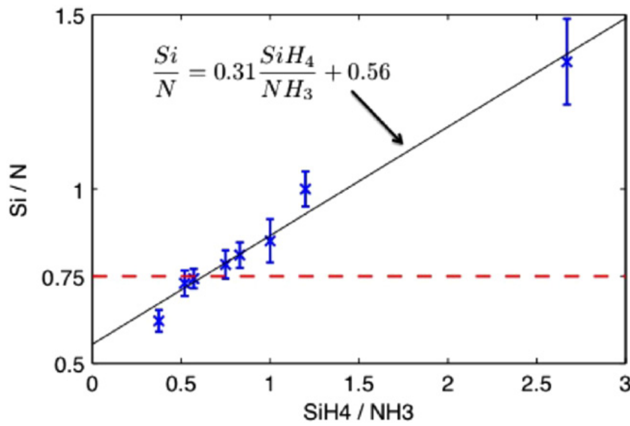

Figure 1. Calculated ratio of Si over N in the grown SiN film as a function of SiH_4/NH_3 precursor ratio used in the PECVD reactor. 0.75 corresponds to stoichiometric Si_3N_4.

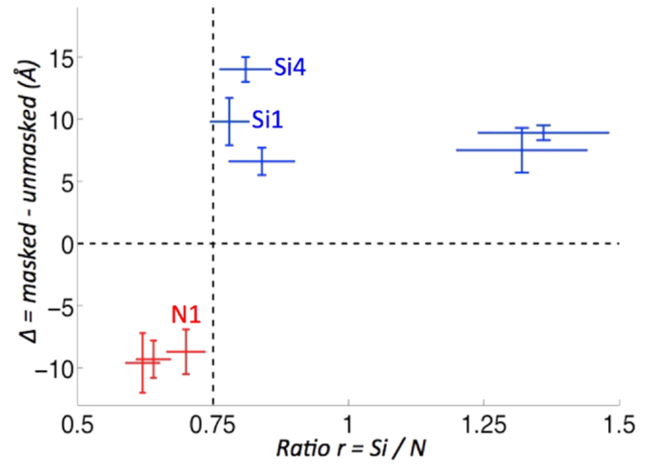

Figure 2. Local control of thickness as a function of the composition of the silicon nitride film, of stoichiometric formula Si_3N_4. In blue, Si-rich $Si_{3+x}N_4$ mask. In red, the $Si_{3+x}N_4$ mask was N-rich.

nitride mask decomposes and vanishes before graphitization is complete. Importantly, the off-stoichiometry of the $Si_{3+x}N_4$ coating controls whether the silicon nitride layer enhances or suppresses graphene growth relative to uncovered areas. We find that N-rich $Si_{3+x}N_4$ masks ($x < 0$) decrease the average number of layers by three compared to uncovered regions while Si-rich silicon $Si_{3+x}N_4(x > 0)$ increase thickness by two to four layers. The graphene layers of samples prepared with nearly stoichiometric Si_3N_4 show good mobilities up to 7100 $cm^2 . V^{-1} . s^{-1}$, with electron concentrations in the 10^{12} cm^{-2} range. Raman spectroscopy and AFM measurements confirm that the graphene grown in areas initially covered by the mask has good structural quality.

After preparation of the surface of 3.5 × 4.5 mm^2 4H-SiC wafer dies by a high temperature hydrogen etch [14], silicon nitride is deposited by low-power plasma-enhanced chemical vapor deposition (PECVD) using SiH_4 and NH_3 as precursor gases. A hard mask (glass slide) covers half the SiC die so that the evaporated SiN layer covers only half the sample. We have confirmed by AFM measurements after removing SiN with hydrofluoric acid (HF) that the plasma does not result in detectable damage to the SiC surface. Patterns of SiN were achieved by standard lithography, using PMMA as the resist, and HF as the etchant (harmless to SiC).

We estimated the stoichiometry of the SiN films as a function of the precursor ratio (SiH_4/NH_3) by measuring the refractive index at 632.8 nm ($n_{632.8}$) of the SiN films with an ellipsometer. Following [15, 16], $n_{632.8}$ is approximately linearly dependent on the ratio Si/N in the deposited film:

$$\frac{\mathrm{Si}}{N} = \frac{n_{632.8} - 1.35}{0.74}. \tag{1}$$

Figure 1 gives a calibration of the SiN composition as a function of the precursor ratio (SiH_4/NH_3) in the PECVD process. The straight line is a linear fit of the data.

The confinement-controlled sublimation (CCS) growth method is used for graphitization [14]. This technique consists in heating a SiC chip in a graphite enclosure connected to a vacuum chamber (about 10^{-5} mbar) by a calibrated hole. This increases the built-in Si partial pressure, which controls the rate of silicon sublimation from the SiC surface, bringing the graphene growth process close to equilibrium.

The growth process consists of 10 min at 800 °C, followed by graphene growth between 1420–1550 °C for 8–20 min. One exception in figure 2 is sample Si4, which after the 800 °C annealing, was held at 1150 °C for 20 min, and then graphitized.

After graphitization the SiN mask has vanished. The Raman spectra show neither the Si–H nor the N–H stretching modes [17], respectively at 2190 and 3360 cm^{-1}, that were observed before growth. AFM images (see figures 3 and 4) show the typical SiC terraces and the typical multilayer epitaxial graphene pleat structure with no AFM nor Raman evidence for left-over SiN in both Si-rich and N-rich cases. The SiN layer is expected to decompose into solid Si and gaseous N2 during the 1150 °C plateau [18–20]. The remaining Si sublimates during graphitization around 1500 °C, consistent with CCS growth [14].

Ellipsometry measurements (Horiba Jobin-Yvon AutoSE) on half-masked samples are reported in figure 2. We used a spot size of 250 × 250 μm^2, and analyzed response in the range 440–850 nm, with a three-term Cauchy model optimized for 4H-SiC and graphene layers [21]. Each thickness reported in figure 2 is the average of 12 measurements, spread on the whole analysed surface. We observe 2–3 additional layers of graphene under the Si-rich initially masked (IM) areas, and consistently 3 fewer layers under the N-rich IM areas, compared to the initially bare (IB) half on each sample. Sample Si4 (Si-rich $Si_{3+x}N_4$ mask), which had an additional higher temperature annealing step at 1150 °C, shows 4–5 additional graphene layers. The increased (reduced) number of graphene layers depending if the mask is over (under) stoichiometric was observed in a total of 20 samples, of which 8 have a precise composition measured as reported in figure 2. Note that the excess number of layers doesn't seem to depend on the over-stoichiometry; however, the over-stoichiometry impacts the quality of the graphene films. For the same growth

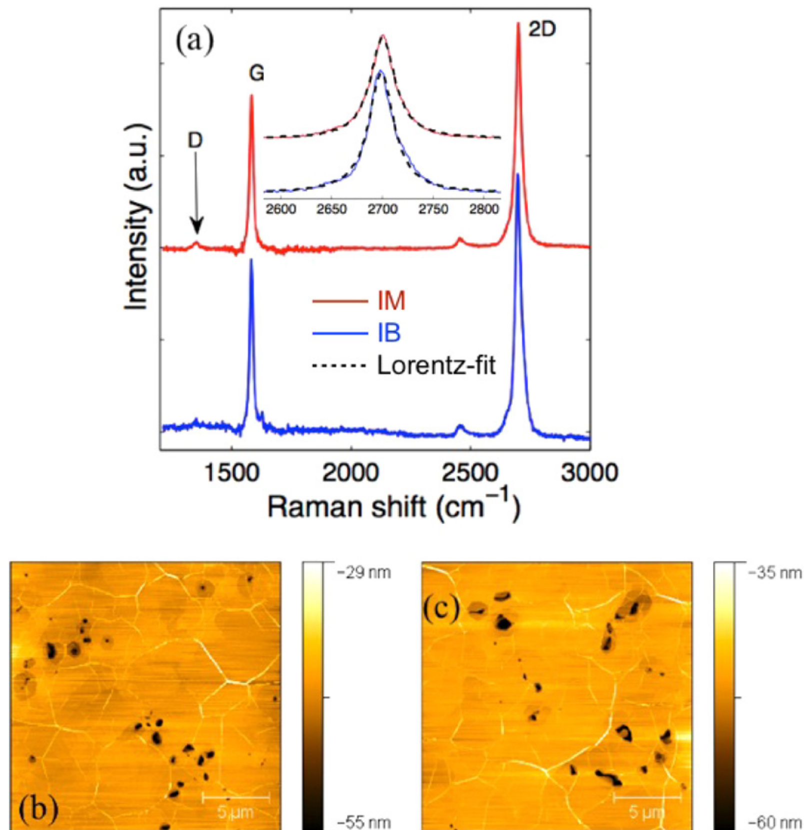

Figure 3. Sample N1, N-rich $Si_{3+x}N_4$ mask. (*a*): Raman spectra (SiC contribution subtracted) of IM and IB areas. (*b*)–(*c*): AFM images of (*b*) IM area and (*c*) IB area (scale $20 \times 20\ \mu m^2$) showing the typical graphene pleat structure observed in MEG samples.

conditions graphene is more disordered for Si-rich SiN, as shown by a higher Raman D peak.

Raman spectra (wavelength 532 nm) and AFM topography images of samples N1 and Si1 are shown in figures 3 and 4, respectively. Of all the samples studied, the silicon nitride films deposited on N1 and Si1 were the closest to stoichiometric Si_3N_4, see figure 2. These samples had the lowest Raman D peaks, sharpest 2D peaks, and smoothest AFM images, and hence were patterned for electronic measurements. More specifically sample N1 was grown for 10 min at 1450 °C and sample S1 for 9 min at 1480 °C; the mask composition for S1 is Si/N = 0.78, and 0.70 for N1; the thickness is 130 nm.

Raman on the IM and IB areas of N1 and on the IM area of Si1 reveals the characteristic graphene peaks, see figures 3 and 4. The graphene 2D and G Raman peaks are clearly identified (the SiC Raman contribution was subtracted). The 2D peak can be fitted by a single Cauchy-Lorentz distribution [22] centered at 2699 cm^{-1} for the IM area of N1 (2700 cm^{-1} and 2689 cm^{-1}, respectively for the IB part of N1 and the IM half of Si1) with FWHM = 29 cm^{-1} (36 cm^{-1} and 29 cm^{-1}, respectively). The D peak at 1350 cm^{-1} is very small, and even undetectable for Si1 and N1. This indicates low defect density in the graphene lattice. For the other samples of figure 2, the 2D peak is centered from 2706 to 2726 cm^{-1}, with FWHM from 52 to 70 cm^{-1}, consistent with 2D MEG [11, 22]. The higher D peaks and the broader blue-shifted 2D peaks (at FWHM 52–70 cm^{-1}) for the other samples referenced in figure 2 reveal respectively smaller domain sizes and compressive strain in the graphene [6, 22]. Specifically, we do not observe the characteristic shouldered 2D peak of highly ordered pyrolitic graphite (HOPG), as already reported for multilayered epitaxial graphene on the C-face [22]. The slight asymmetry of the IB 2D peak in figure 3(*a*) may be due to a variation of strain in the graphene stack or a small fraction of Bernal stacking fault [6, 23]. MEG on SiC with a 2D-FWHM of 58 cm^{-1} [11], 68 cm^{-1} [24] have already been reported.

The AFM images of figures 3 and 4 confirm the presence of graphene, as shown by the MEG characteristic pleat structure [14]. In the graphitized areas, the AFM images in figures 3(*b*) and (*c*) and 4(*b*) have comparable characteristics in terms of pleat structure, including pleat height (1.5–2.4 nm), pleat surface density and semi hexagonal orientation. Sample Si1 is particularly interesting in that while the IM area is fully coated with graphene with an average of 3 layers, the IB area is essentially not graphitized, as seen in the Raman spectra, ellipsometry and AFM images. On the AFM image of figure 4(*c*), a bare SiC step structure can be observed, which is confirmed by Raman spectroscopy, see figure 4(*a*). MEG growth is observed in some spots, most probably initiated at screw dislocations in SiC, as already observed [6, 25]. This indicates selective growth, with graphene where the mask was, and almost no graphene elsewhere.

Hall bars (5 μm long, 3.5 μm wide) were patterned in sample Si1 and N1 using electron beam lithography, oxygen plasma etching and Ti/Pd/Au contacts (thickness 0.5/20/40 nm). From room temperature Hall and magnetoresistance measurements

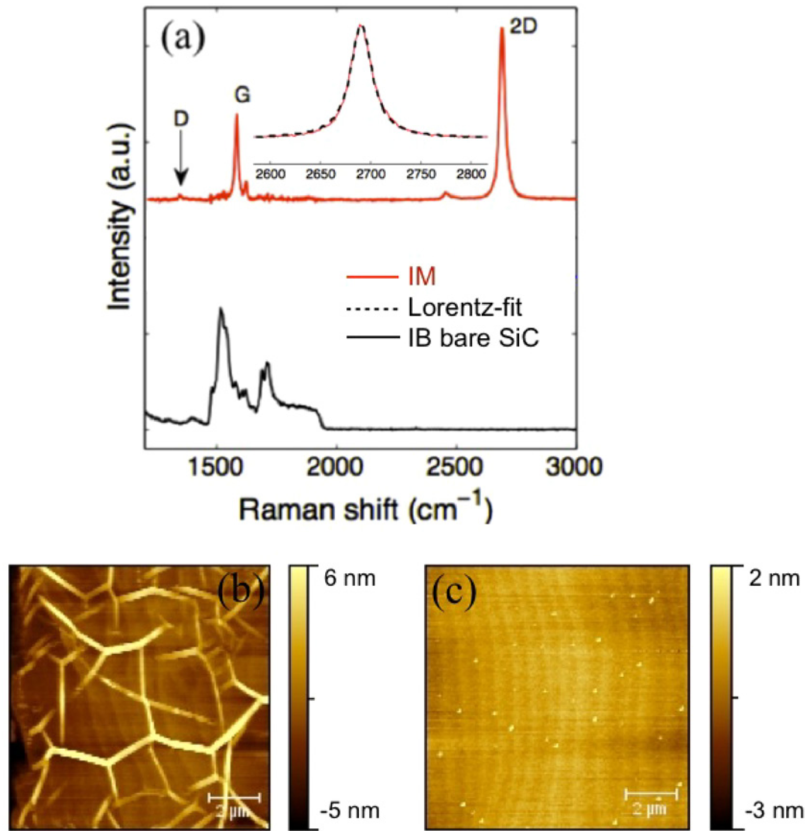

Figure 4. Sample Si1, Si-rich SiN mask. (*a*): Raman spectra (SiC contribution subtracted), showing the typical MEG spectrum. For the Raman spectrum the intensity is normalized to the SiC plateau at 1900 cm^{-1}. Note the quasi absence of D-peak. (*b*) and (*c*): AFM image of (*b*) IM area (scale 10×10 μm^2), and (*c*) IB area (scale 10×10 μm^2).

(figure 5), electronic mobilities are found between 3200 and 7100 $cm^2 \cdot V^{-1} \cdot s^{-1}$, and carrier concentrations are in the 10^{12} cm^{-2} range, showing excellent graphene quality.

As a demonstration of the capability of the method, graphene has been selectively grown in the shape of Buzz, Georgia Tech's mascot. Figure 6 demonstrates that the submicrometer resolution of the SiN mask pattern (figure 6(*a*)) is directly transferred to the selectively grown graphene, as shown by optical contrast (figure 6(*b*)) and Raman spectroscopy maps of the characteristic 2D and G graphene peaks. The optical image correlates nicely with the Raman maps, as expected for graphene on SiC [26]. The absence of 2D peak in the grey areas of figure 6(*c*) demonstrates selectivity.

The main result of this study is that the presence of a silicon nitride mask evaporated on silicon carbide prior to graphitization enhances (Si-rich $Si_{3+x}N_4$ mask, $x > 0$) or reduces (N-rich $Si_{3+x}N_4$, $x < 0$) the number of layers grown compared to uncovered areas. Control samples, grown in the same condition but with no mask, have the same number of layers (within one layer) as the IB areas.

A simple explanation for the reduction of the number of layers under the N-rich masks would be that graphitization is delayed under the mask, starting only after SiN decomposition. It is known that capping SiC with an AlN mask, that doesn't evaporate, prevents graphene formation [11]. More surprising is the enhanced number of layers under the Si-rich mask. A possibility is that Si dangling bonds present in the Si-rich-SiN mask [27–30] react with SiC. The role of Si in promoting the growth of graphene was demonstrated by implantation of Si in SiC. The implanted SiC surface results in graphene formation at lower temperature than pristine SiC [12]. Si dangling bonds at SiN_3 sites have already been proposed as the dominant defects in Si-rich and stoichiometric PECVD silicon nitride, acting as amphoteric traps [29]. Moreover, in N-rich films, electron spin resonance (ESR) studies have shown that the density of these defects is greatly reduced or even suppressed [31], making N-rich $Si_{3+x}N_4$ a better dielectric than Si-rich $Si_{3+x}N_4$ films. However the exact mechanism per which the growth is enhanced will require far more study. The decomposition of SiC and graphene growth is not well understood even in the simple case of a bare SiC surface. For instance the growth rate is extremely slow on the Si-face but is much faster on the C-face. Out-diffusion of silicon is clearly the key, pointing to the role of Si in the capping SiN mask.

We have shown that, by using a SiN vanishing mask evaporated onto SiC prior to graphitization, the number of graphene layers varies between masked and non-masked areas. Depending on its chemical composition (Si- rich or N-rich) the $Si_{3+x}N_4$ mask acts as an enhancer or inhibitor of graphene growth (of the order of $+/-3$ graphene layers with the present growth conditions). Areas with and without few layer graphene can therefore be produced side by side during the

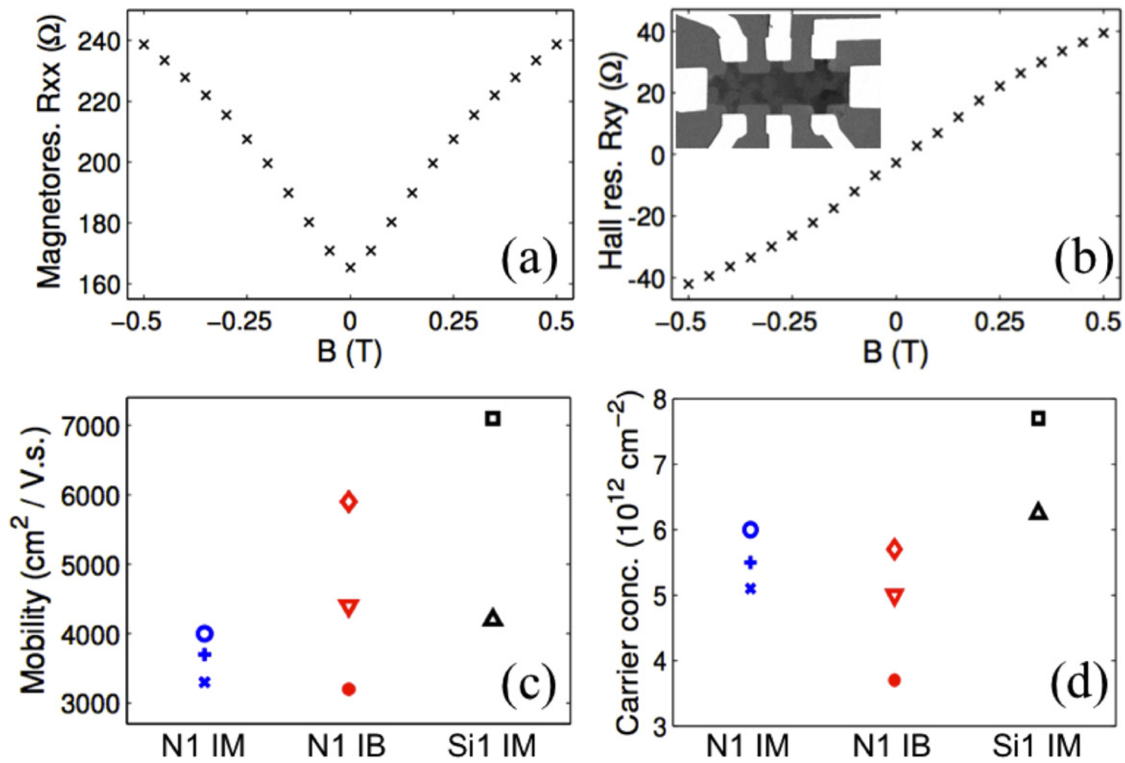

Figure 5. (*a*) and (*b*): Magneto- and Hall resistances at room temperature of IM area of Si1: $n = 7.7\ e^{12}\ cm^{-2}$ and $\mu = 7100\ cm^2 . V^{-1} . s^{-1}$. Hall bar (SEM picture in the inset) is 3 μm wide. (*c*) and (*d*): Mobility and carrier concentrations at room temperature measured on the IM area of N1, IB area of N1, and IM area of Si1.

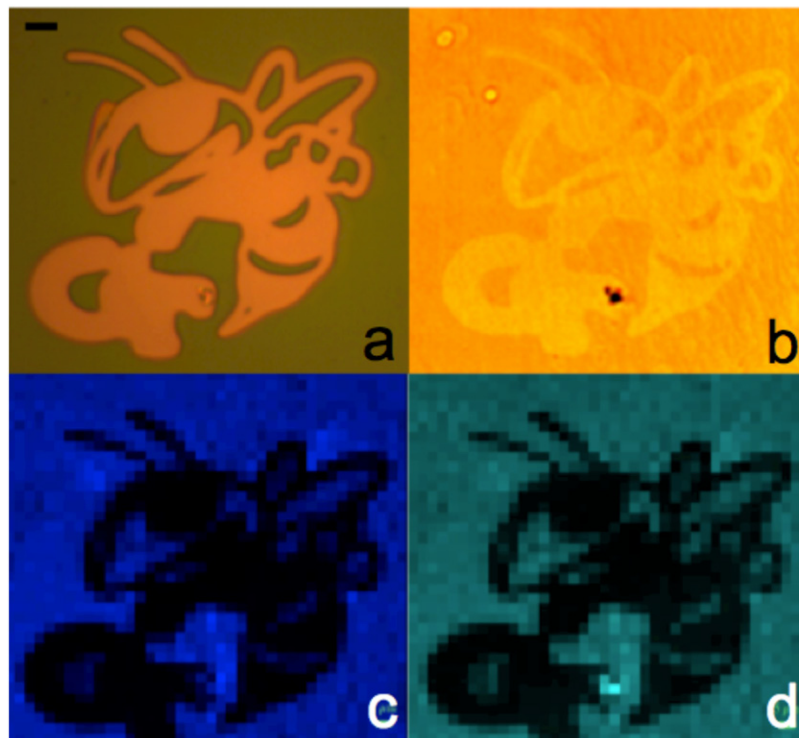

Figure 6. Buzz-of-principle, MEG on SiC using Si-rich SiN mask, demonstrating sub-micron resolution. (*a*): SiN pattern. (*b*): Subsequent MEG growth on SiC, contrast-enhanced optical image. (*c*): Raman 2D map. d: Raman 2D/G map. Scale bar is 10 μm.

heating process. The mask evaporates during graphene growth so that patterned, mask-free graphene layers are obtained directly in a single heating step.

This is a very simple yet potentially quite powerful method to obtain clean resist-free patterned graphene structures. In a further development, the process can in principle be integrated

with carbon contacts deposited prior to graphitization [32]; in a one step process graphene is grown where desired contacts are provided by the predeposited (thermally stable) carbon pads. This provides clean graphene, ready for transport measurements, with no further processing. Moreover the pre-defined growth location may help solve a long-standing problem of patchy growth for single layer areas on the C-face. For instance, using adjacent Si-rich and N-rich masked areas could allow to reach growth selectivity at the monolayer level. This is particularly important for quantum Hall effect metrology applications, which could benefit from large clean single layers on the C-face that has a much higher mobility [6] than the Si-face generally used.

Acknowledgments

The authors thank the French Lorraine Region, W M Keck Foundation, the National Science Foundation (DMR-0820382), the Air Force Office of Scientific Research for financial support and the Partner University Fund for a travel grant. We also acknowledge funding from the Graphene Flagship European program. At last my special thanks to J P Turmaud, X Yang, A Savu, Y Hu, F Zaman, S Bryan, R Dong, T Guo, M Ruan, B Zhang, M Sprinkle, J Hicks, M Nevius, F Wang and O Vail for training, technical support and fruitful discussions.

References

[1] Baringhaus J *et al* 2014 *Nature* **506** 349–54
[2] Hicks J *et al* 2013 *Nat. Phys.* **9** 49–54
[3] Tzalenchuk A, Lara-Avila S, Kalaboukhov A, Paolillo S, Syvajarvi M, Yakimova R, Kazakova O, Janssen T J B M, Fal'ko V and Kubatkin S 2010 *Nat. Nanotechnol.* **5** 186–9
[4] Lin Y M, Dimitrakopoulos C, Jenkins K A, Farmer D B, Chiu H Y, Grill A and Avouris P 2010 *Science* **327** 662
[5] Guo Z *et al* 2013 *Nano Lett.* **13** 942–7
[6] Hu Y, Ruan M, Guo Z, Dong R, Palmer J, Hankinson J, Berger C and de Heer W A 2012 *J. Phys. D: Appl. Phys.* **45** 154010
[7] Orlita M, Faugeras C, Grill R, Wysmolek A, Strupinski W, Berger C, de Heer W A, Martinez G and Potemski M 2011 *Phys. Rev. Lett.* **107** 216603
[8] Dlubak B *et al* 2012 *Nat. Phys.* **8** 557–61
[9] Berger C *et al* 2004 *J. Phys. Chem.* B **108** 19912–6
[10] Lin Y M *et al* 2011 *Science* **332** 1294–7
[11] Rubio-Roy M, Zaman F, Hu Y, Berger C, Moseley M, Meindl J and de Heer W 2010 *Appl. Phys. Lett.* **96** 082112
[12] Tongay S, Lemaitre M, Fridmann J, Hebard A F, Gila B P and Appleton B R 2012 *Appl. Phys. Lett.* **100** 073501
[13] Sprinkle M, Ruan M, Hu Y, Hankinson J, Rubio-Roy M, Zhang B, Wu X, Berger C and de Heer W A 2010 *Nat. Nanotechnol.* **5** 727–31
[14] de Heer W, Berger C, Ruan M, Sprinkle M, Li X, Hu Y, Zhang B, Hankinson J and Conrad E 2011 *Proc. Natl Acad. Sci.* **108** 16900–5
[15] Piggins N, Davis E and Bayliss S 1987 *J. Non-Cryst. Solids* **97–8** 1047–50
[16] Claassen W, Valkenburg W, Habraken F and Tamminga Y 1983 *J. Electrochem. Soc.* **130** 2419–23
[17] Bandet J, Despax B and Caumont M 1999 *J. Appl. Phys.* **85** 7899–904
[18] Singhal S 1976 *Ceram. Int.* **2** 123–30
[19] Hincke W and Brantley L 1930 *J. Am. Chem. Soc.* **52** 48–52
[20] Herrmann M, Schuber C, Rendtel A and Hubner H 1998 *J. Am. Ceram. Soc.* **81** 1095–108
[21] Average thicknesses obtained by ellipsometer match other thickness measurements, notably light absorption (to be published)
[22] Faugeras C, Nerriere A, Potemski M, Mahmood A, Dujardin E, Berger C and de Heer W A 2008 *Appl. Phys. Lett.* **92** 011914
[23] Hicks J, Shepperd K, Wang F and Conrad E H 2012 *J. Phys. D: Appl. Phys.* **45** 154002
[24] Sharma N, Oh D, Abernathy H, Liu M, First P N and Orlando T M 2010 *Surf. Sci.* **604** 84–8
[25] Hite J K, Twigg M E, Tedesco J L, Friedman A L, Myers-Ward R L, Eddy C R Jr and Gaskill D K 2011 *Nano Lett.* **11** 1190–4
[26] Tiberj A, Camara N, Godignon P and Camassel J 2011 *Nanoscale Res. Lett.* **6** 478
[27] Robertson J 1983 *J. Appl. Phys.* **54** 4490–3
[28] Robertson J and Powell M 1984 *Appl. Phys. Lett.* **44** 415–7
[29] Lau W, Fonash S and Kanicki J 1989 *J. Appl. Phys.* **66** 2765–7
[30] Warren W, Robertson J and Kanicki J 1993 *Appl. Phys. Lett.* **63** 2685–7
[31] Jousse D, Kanicki J, Krick D and Lenahan P 1988 *Appl. Phys. Lett.* **52** 445–7
[32] Palmer J, Kunc J, Hu Y, Hankinson J, Guo Z, Berger C and de Heer W A 2014 *Appl. Phys. Lett.* **105** 023106

Copyright of Journal of Physics: D Applied Physics is the property of IOP Publishing and its content may not be copied or emailed to multiple sites or posted to a listserv without the copyright holder's express written permission. However, users may print, download, or email articles for individual use.